

A Concatenated Multitone Multiple Antenna Scheme for Multiuser Uplink Communications

Andrea M. Tonello, *Member, IEEE*

DIEGM - Dipartimento di Ingegneria Elettrica Gestionale e Meccanica
Università di Udine
Via delle Scienze 208 - 33100 Udine - Italy
e-mail: tonello@uniud.it

Abstract— In this paper, we describe a transmission technology approach for application in asynchronous multiuser wireless channels, i.e., reverse link. The scheme is based on the concatenation of multitone modulators with transmission over multiple antennas. It implements a form of space-frequency division multiplexing. Its efficient realization can be done via FFT and poly-phase low-rate filtering. The design parameters are flexible and are chosen to cope with the users' time and frequency offsets, as well as with the time-frequency channel selectivity. We also apply outer direct sequence data spreading, and frequency hopping to obtain improved diversity gains and interference averaging benefits. The key aspect of the proposed asynchronous multitone multiple antenna air-interface is its intrinsic robustness to multiple access interference, and channel time-frequency selectivity.

Index Terms— Concatenated multitone modulation, DMT modulation, FMT modulation, Multiple access, Multiple transmit antennas, Multiuser MIMO systems, MIMO OFDM.

I. INTRODUCTION

IN this paper, we present a proposal for an uplink air-interface that combines multitone modulation with multiple antenna transmission. The air-interface approach that we describe is intended for application in both cellular and wireless LAN scenarios. We point out that, currently, wireless LAN technology (IEEE 802.11a and Hiperlan II) deploys 20 MHz channels supporting data rates up to 54 Mbps, while 3G cellular technology (UMTS, CDMA 2000) deploys 5 MHz channels supporting data rates up to 2 Mbps (up to 10 Mbps in downlink high-speed data packet access recent releases). The gap in offered data rates between the two technologies is quite significant. Different available spectrum, and different mobility and coverage requirements in part justify it. It is indeed of great importance to increase current cellular data rates to bridge the gap with WLAN technology and, of more importance, to increase spectral efficiency. Besides the 3G spectrum limitation, the design of an air interface for a cellular system has to encompass challenging technical requirements such as

high mobility, and high coverage. Most of the work has focused on improvements for the forward link rather than the reverse link. This is justified by the general opinion that the traffic is asymmetric since most high-speed services are required in the downlink only, e.g., file downloading, and voice/video streaming services. Indeed, it has to be said that the reverse link of a cellular system poses further challenges that are due to the asynchronous nature of this link. That is, the communication channels of distinct users can be considered independent, and experience propagation delays, carrier frequency offsets, Doppler from movement, and transmission power limitations. These impairments/limitations translate into multiple access interference (MAI) that may severely affect and limit performance. This is a well understood problem, for instance, in CDMA like type of technology that can be mitigated only with the deployment of complex multiuser receivers. It is therefore evident that a technology that allows for deep multiuser interference reduction, and that requires moderate receiver complexity is of great importance.

The uplink air-interface that we describe in this paper is based on multicarrier modulation. Multicarrier modulation is a mature technology that has proven to be effective in simplifying the equalization task in severely dispersive fading channels. In particular orthogonal frequency division multiplexing (OFDM) has been chosen in 802.11a and Hiperlan II together with a time division multiple access scheme. When multiplexing is done in a time division fashion, the exploitation of the system resources may not exhibit sufficient granularity as required in multiuser bursty and heterogeneous traffic. In other words a combination of both time division and frequency division multiplexing can show better available resource utilization [17]. However, it should be noted that OFDM, referred to as discrete multitone (DMT) modulation in this paper, is severely affected by time misalignments and carrier frequency offsets that can be large in a cellular, high mobility environment. This is due to the fact that in conventional OFDM, sub-channels exhibit *sinc* like frequency response, therefore their orthogonality can be easily lost in the absence of precise synchronization [13]-[15]. In an asynchronous multiuser environment, increased robustness and better performance can be obtained

Part of this work was supported by MIUR under project FIRB "Reconfigurable platforms for wideband wireless communications", prot. RBNE018RFY.

with filtered multitone (FMT) modulation architectures where the sub-channels are shaped with appropriate time-frequency concentrated pulses [1], [10], [13], [14].

A. Proposed Multitone Multiuser Approach

In the uplink air-interface herein described, users are multiplexed in a frequency division fashion through the serial concatenation of two multicarrier modulators (Fig. 1, and Fig. 2). This idea was recently proposed in [9]. However, in [9] we did not consider any type of space-time coding. Instead, in this paper we assume the users' transmitter to be equipped with N_T antennas. The inner module is an FMT modulator that efficiently performs frequency division multiplexing of the users. In the outer module we combine a modified DMT modulator with orthogonal direct sequence (DS) data spreading. The outer module behaves as a transmit diversity scheme and is used to exploit space-frequency diversity [2], [8]. We refer to the outer modulator as orthogonal space-time cyclically prefixed discrete multitone (O-ST-CP-DMT) modulator [8]. It essentially works as the cyclic delay diversity scheme that is also described in [2].

Transmission over each antenna is accomplished with an inner modulator that is based on an FMT approach with M sub-channels. It is used for users' channelization, i.e., to split the available spectrum into slices that are assigned to distinct users [10]. A user in a cell (sector) can be assigned with one or more inner sub-channels according to its data rate requirement. The N_T antenna signals of a given user are simultaneously transmitted (by the antennas), and occupy the spectrum corresponding to the assigned inner sub-channels (Fig. 1). Each inner sub-channel is shaped with a filter having frequency concentrated response, e.g., a squared root raised cosine pulse. An appropriate frequency guard is set in order to enhance frequency separation of the inner sub-channels. Thus, the presence of time misalignments across users, and channel time dispersion does not compromise the orthogonality of the users' channels. Further, the frequency guards yield protection against carrier frequency offsets that may exist between users.

We emphasize that in our design the number of inner sub-channels may not be large enough to obtain a sub-channel bandwidth smaller than the coherence bandwidth. Hence, each inner sub-channel does not exhibit a flat frequency response and some residual intersymbol interference (ISI) arises. The outer O-ST-CP-DMT modulator uses M_2 tones and is applied serially over each inner sub-channel. It removes the residual ISI, so that we obtain a flat frequency response for each inner sub-channel. Further, it orthogonalizes the N_T spatial channels differently from other DMT (OFDM) multiple antenna schemes [5], [6]. That is, it transforms the multiple transmit antenna system into a single transmit antenna system that is characterized by a modified transfer function [2], [8].

In this paper, we carry out a detailed system analysis to show that, under certain conditions, the serial concatenation of the outer O-ST-CP-DMT modulator, the inner FMT modulator, and the N_T transmit antennas, can be viewed as generating MM_2 orthogonal sub-channels over which up to M users are

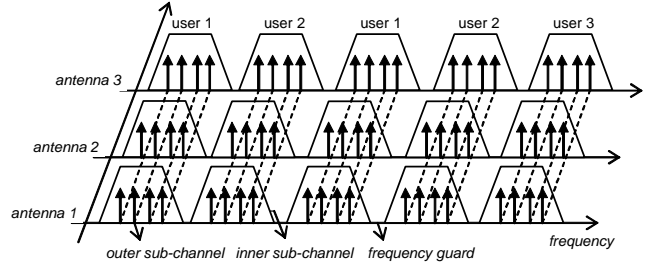


Fig. 1. Space-Frequency user channelization via inner FMT concatenated with outer DMT, and transmission over multiple antennas.

TABLE I ACRONYMS AND NOTATION	
DMT	Discrete multitone modulation (OFDM).
FMT	Filtered multitone modulation.
O-ST-CP-DMT	Orthogonal space-time cyclically prefixed discrete multitone modulation.
N_T	Number of transmit antennas.
M	Number of tones of inner modulator.
N_U	Number of users.
M_u	Number of inner sub-channels assigned to user u .
M_2	Number of tones of outer modulator.
$N = M_2 + \mu$	$\mu \geq 0$ cyclic prefix outer modulator.
T	Transmission period.
$W = 1/T$	Nominal overall system bandwidth.
$\Delta f = 1/MT$	Inner sub-channel spacing.
$T_0 = MT(1 + \alpha)$	Inner sub-channel symbol period with $\alpha \geq 0$.
$T_1 = NT$	Outer sub-channel symbol period.
$g(nT)$	Prototype filter of inner sub-channel.

multiplexed. Each sub-channel can support a peak rate that is in order of $W/(MM_2)$ symb/s where W is the overall system bandwidth. Sub-channels do not overlap, and exhibit a flat frequency response. More important, the rank of the multiple antenna frequency selective channel is not altered with the proposed architecture.

To exploit diversity each user can deploy direct sequence data spreading (DS-SS) across its assigned sub-channels [3]. Note that DS spreading does not decrease the transmission data rate. Further, since the outer sub-channels exhibit a flat frequency response, detection complexity can be kept small. It can be performed through a zero forcing (ZF), or minimum mean square error (MMSE) approach.

Finally, in the architecture that we propose adaptive allocation of sub-channels to users (in a frequency hopping fashion) can be supported [9].

The overall transmit-receive architecture can be efficiently implemented via fast Fourier transforms (FFT), and polyphase filtering. Its key design aspects are the choice of the partitioning of the tones across the concatenated modulators and the antennas, the tone spacing, and the optimization of the sub-channel shaping pulses. These parameters are determined by the desired characteristics in terms of resources granularity, immunity to propagation delays, carrier frequency offsets, channel Doppler spread and delay spread. As an example, we describe the application of the proposed air-interface to a 3.84 MHz channel. However, the air interface can be upgraded to support wider bandwidths.

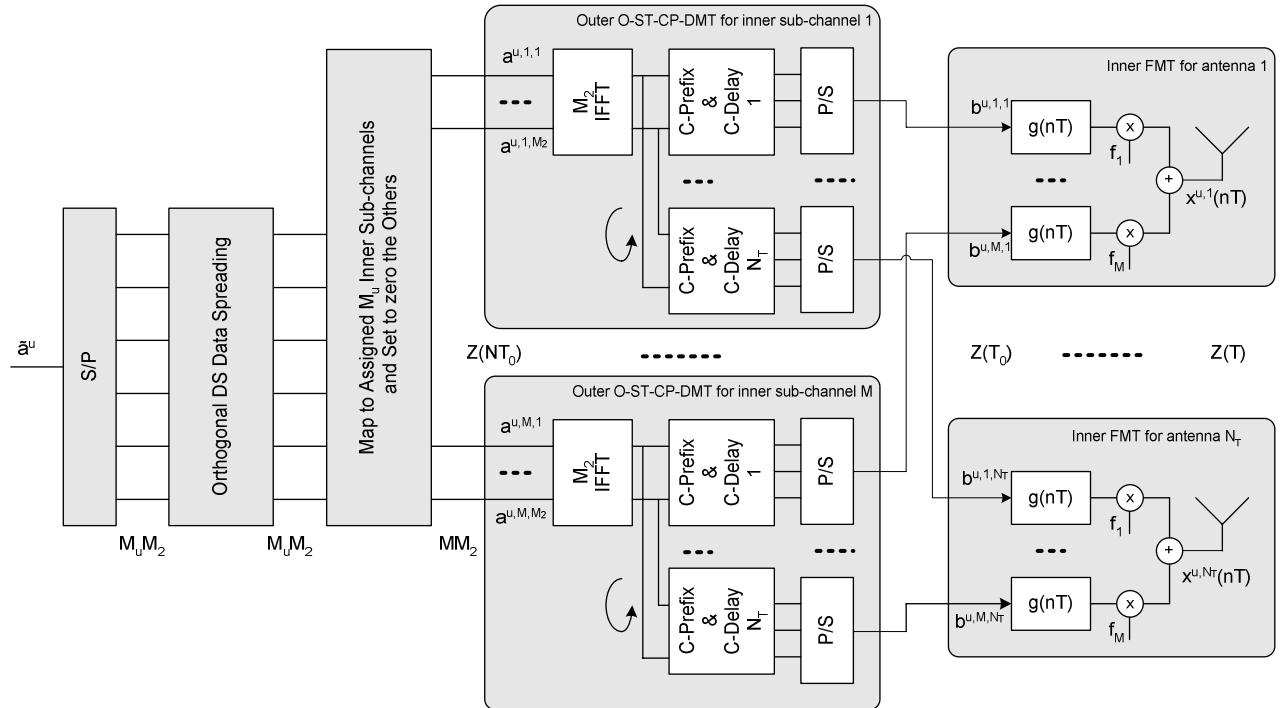


Fig. 2. Base-band discrete-time transmitter of user u .

II. TRANSMISSION CHAIN FOR THE CONCATENATED SPACE-TIME MULTITONE MODULATED MULTIUSER SYSTEM

In this section we describe the key components of the proposed multiuser system. In Table I we report acronyms and notation, while in Fig. 2 we depict the transmitter of a given user. It combines the idea of concatenating two multitone modulators as illustrated in [9] with the idea of performing spatial data multiplexing as illustrated in [8]. We start from the inner FMT modulator, then we describe the outer O-ST-CP-DMT modulator, and finally the DS data spreading stage. We choose this order because the system is modular, and can work with the inner modulator only.

A. Inner FMT Modulator, User Multiplexing, and Multiple Transmit Antennas

We assume to have N_T transmit antennas per user. Transmission over each antenna is accomplished with an inner FMT modulator having M tones. It is used for users' channelization, i.e., to split the available spectrum into slices that are assigned to distinct users [10], [14]. A given user in a given cell (sector) can be assigned with one or more inner sub-channels according to its data rate requirement. Each inner sub-channel is shaped with a filter having frequency concentrated response, e.g., a squared root raised cosine (s.r.r.c) pulse with roll-off α_1 . The inner sub-channels are centered at frequency f_k , with separation $f_k - f_{k-1} = 1/MT$, and have Nyquist bandwidth equal to $1/T_0$ with $T_0 = MT(1 + \alpha)$, and $\alpha = \alpha_1 + \alpha_2$. If distinct users deploy non overlapping (in frequency) sub-channels, users' orthogonality is achieved even in the presence of time misalignments across users, and channel time disper-

sion. We choose, in fact, $\alpha_2 > 0$ such that an appropriate frequency guard exists between adjacent sub-channels. This yields protection against carrier frequency offsets across users. Therefore perfect orthogonality between asynchronous users can be achieved, in principle, with confined sub-channels and frequency offsets between users smaller than α_2/T_0 (see next Section).

The N_T antenna signals of a given user are simultaneously transmitted (by the antennas), and occupy the spectrum corresponding to the assigned inner sub-channels (Fig. 1). The low-pass discrete-time signal transmitted by user u over antenna $t = 0, \dots, N_T - 1$, can be written as

$$x^{u,t}(nT) = \sum_{k=0}^{M-1} \sum_{l \in \mathbb{Z}} b^{u,k,t}(lT_0) g(nT - lT_0) e^{j \frac{2\pi}{M} nk}. \quad (1)$$

$b^{u,k,t}(lT_0)$ denotes the symbol transmitted by user u over the inner sub-channel $k = 0, \dots, M-1$, and antenna t , at time lT_0 . Distinct inner-sub-channels can be assigned to distinct users. Thus, for the unassigned inner sub-channels, the symbols are set to zero,

$$b^{u,k,t}(lT_0) = 0 \quad \text{for } k \notin K_u \quad (2)$$

where K_u denotes the set of M_u sub-channel indices that are assigned to user u .

Note that there is one FMT modulator per transmit antenna. Each can be efficiently implemented with an inverse fast Fourier transform (IFFT). The outputs of the IFFT are low-rate filtered with sub-channel pulses that are obtained from the polyphase decomposition of the prototype pulse $g(nT)$ [1], [8].

The complex symbols $b^{u,k,t}(IT_0)$ belong to the PSK/QAM constellation unless the outer O-ST-CP-DMT modulator is used. In this case, the symbols $b^{u,k,t}(IT_0)$ are obtained by an outer DMT transform as explained in the next sub-section.

B. Outer Space-Time Orthogonal DMT Modulator

The outer modulator is a modified discrete multitone (DMT) modulator with M_2 tones that is applied serially over each inner sub-channel [2], [8] (Fig. 2). It is here referred to as orthogonal space-time cyclically prefixed DMT (O-ST-CP-DMT). It is used to obtain both a flat frequency response for each inner sub-channel, and to orthogonalize the spatial channels. We emphasize that in our design the number of inner sub-channels may not be large enough to obtain a sub-channel bandwidth smaller than the coherence bandwidth. Further, transmission by the antennas of a user is simultaneous, and occupies the same portions of the spectrum (inner sub-channels).

The outer O-ST-CP-DMT modulator works as follows. For user u , and inner sub-channel k , we take a block of M_2 symbols that belong to the PSK/QAM constellation (unless direct sequence data spreading is applied as described in the next sub-section). The block of symbols is denoted as

$$a^{u,k,k'}(mNT_0) \quad \text{for } k' = 0, \dots, M_2 - 1. \quad (3)$$

The block has transmission period $T_1 = NT_0$, with $N = M_2 + \mu$. $\mu \geq 0$ denotes an appropriate cyclic prefix that is used to counteract the channel time dispersion due to frequency selectivity (see below). Each block is transformed by an M_2 points IFFT. A cyclic prefix of length μ is added to generate an output block of N symbols. Finally, the output block is transmitted by an antenna after the insertion of a cyclic delay. The number of outer tones is chosen to fulfill the following relation $M_2 \geq \mu + N_T - 1$, with μT_0 larger than the maximum inner sub-channel time dispersion. In formulae, starting from the block (3), we generate N_T blocks of N symbols each as follows

$$b^{u,k,t}(IT_0) = b^{u,k,t}(nT_0 + mNT_0) = \sum_{k'=0}^{M_2-1} a^{u,k,k'}(mNT_0) e^{j\frac{2\pi}{M_2}(n-\mu-t\delta)k'} \quad (4)$$

for $t = 0, \dots, N_T - 1$, $l = n + mN$, $n = 0, \dots, N - 1$, and $m \in \mathbb{Z}$. δ is an appropriately chosen integer delay. Assuming $\delta = 1$, the output of (4) can be collected in the following $N_T \times N$ matrix

$$N_T \updownarrow \begin{bmatrix} b_{M_2-\mu} & b_{M_2-\mu+1} & \dots & b_{M_2-1} & b_0 & b_1 & \dots & b_{M_2-1} \\ b_{M_2-\mu-1} & b_{M_2-\mu} & \dots & b_{M_2-2} & b_{M_2-1} & b_0 & \dots & b_{M_2-2} \\ \dots & \dots & \dots & \dots & \dots & \dots & \dots & \dots \\ b_{M_2-\mu-N_T+1} & \dots & \dots & b_{M_2-N_T} & b_{M_2-N_T+1} & \dots & \dots & b_{M_2-N_T} \end{bmatrix} \leftarrow \begin{matrix} \longrightarrow \\ N \end{matrix}$$

where $b_n = \sum_{k'=0}^{M_2-1} a^{u,k,k'}(mNT_0) e^{j2\pi nk'/M_2}$. The rows are transmitted by distinct antennas.

Note that the symbol stream (4) is fed to the inner modula-

tor. In particular, the symbol stream $b^{u,k,t}(IT_0)$ of indices (u, k, t) belongs to user u , and is transmitted over inner sub-channel k by the t -th antenna. According to (3), and (4), $a^{u,k,k'}(mNT_0)$ is the data symbol transmitted by user u over the outer sub-channel k' that falls within the inner sub-channel k , at time mNT_0 .

The O-ST-CP-DMT transform can be viewed as a rate one ST block code. Thus, including the cyclic prefix penalty, the inner sub-channel k supports a net symbol rate of M_2 / NT_0 symb/s.

C. Direct Sequence Data Spreading

To exploit diversity we consider the deployment of outer DS data spreading [3] (DS-CDMA). That is, starting from a PSK/QAM data symbol stream of a given user, we generate the blocks of symbols in (3) using DS data spreading. The procedure works as follows.

Let $M_u \geq 1$ be the number of inner sub-channels that is assigned to user u . Thus, if M_2 is the number of outer-sub-channels, user u has available $L = M_u M_2$ overall channels. Let $\tilde{a}^{u,i}(mNT_0)$, $i = 0, \dots, L - 1$ be its PSK/QAM data symbols to be transmitted over the L channels at time mNT_0 . Then, we apply a Walsh-Hadamard orthonormal transform to generate the block of symbols

$$a^{u,k,k'}(mNT_0) = \sum_{i=0}^{L-1} \tilde{a}^{u,i}(mNT_0) c(i, kM_2 + k') \quad (5)$$

for $k = 0, \dots, M_u - 1$, $k' = 0, \dots, M_2 - 1$, that are then fed to the O-ST-CP-DMT modulator. In (5) $c(i, j)$ for $j = 0, \dots, L - 1$ denotes the elements of the i -th row of an orthonormal matrix of size L .

The above procedure does not add redundancy, i.e., we keep the symbol rate equal to M_2 / NT_0 symb/s per inner-sub-channel. Further, we note that the same codes can be assigned to all inner sub-channels, and users if they transmit over distinct channels. It implements space-frequency spreading by partitioning a spreading sequence over space and frequency. In Section V we report several performance results to show the improvements due to the space-frequency diversity exploitation.

III. ASYNCHRONOUS MULTIPLE ACCESS CHANNEL AND DEMODULATION STAGES

In this section we describe the demodulation process assuming an uplink scenario. It comprises a stage for demodulation of the inner FMT module, a stage for demodulation of the outer O-ST-CP DMT module, and finally a stage for data despreading.

A. Uplink Channel

The signals of N_U users propagate through independent time-variant frequency selective fading channels. We assume an equivalent discrete-time lowpass channel model that results from the concatenation of the DAC transmit filter, the channel, and the ADC receive filter. If the channel is slow with respect to the length of the ADC filter, the composite lowpass received signal of antenna r can be written as follows [10]-[12]

$$y^r(iT) = w^r(iT) + \sum_{u=1}^{N_U} \sum_{t=0}^{N_T-1} \sum_{k=0}^{M-1} \sum_{l \in \mathbb{Z}} b^{u,k,t}(lT_0) \sum_{n \in \mathbb{Z}} \{g(nT - lT_0) \times g_{ch}^{u,t,r}(iT - nT - \Delta t_{u,k,t,r}; iT) e^{j[2\pi(\frac{nk}{M} + \Delta f_{u,k,t,r} iT) + \phi_{u,k,t,r}]}\}. \quad (6)$$

The above model is based on the following assumptions:

- N_T transmit antennas, and N_R receive antennas.
- $g_{ch}^{u,t,r}(mT; iT)$ is the equivalent lowpass time-variant channel impulse response that comprises the DAC-ADC filters for the t -th transmit $- r$ -th receive antenna link of user u .
- $\Delta t_{u,k,t,r}$ is the time offset due to the propagation delay of user u , inner sub-channel k , and antenna link (t, r) .
- $\Delta f_{u,k,t,r}$ is the frequency offset of user u , inner sub-channel k , and antenna link (t, r) that is due to Doppler, and misadjusted oscillators. It is assumed much smaller than $1/T$.
- $\phi_{u,k,t,r}$ is the phase offset of user u , inner sub-channel k , and antenna link (t, r) .
- $w^r(iT)$ is a sequence of i.i.d. zero mean Gaussian random variables.

We herein consider a three stage receiver that first performs demodulation for the inner FMT modulator, then accomplishes O-ST-CP-DMT demodulation for each inner sub-channel, and finally it runs despreading and data decision. For ease of notation, we further assume the time offsets, frequency offsets, and phase offsets to be identical for all transmit antenna links, i.e.,

- $\Delta t_{u,k,t,r} = \Delta t_{u,k}$, $\Delta f_{u,k,t,r} = \Delta f_{u,k}$, $\phi_{u,k,t,r} = \phi_{u,k}$ for all antennas links.

B. Inner FMT Demodulation Stage

Multiuser FMT detection is accomplished by acquiring time, and frequency synchronization with each active user, and running a bank of front-end matched filters that are matched to the individual sub-channels. The matched filter outputs are sampled at rate $1/T_0$. Finally, multi-channel equalization is in general required [10], [12]. Under certain conditions, the optimal FMT detector simplifies into a bank of independent equalizers, one for each inner sub-channel [10]. Since transmission by the antennas is simultaneous, each inner sub-channel detector needs to perform space-time equalization [8], [11]. However, as we will show in what follows, the outer O-ST-CP-DMT modulator orthogonalizes both the ISI channel and the multiple transmit antenna channel, such that detection simplifies into one-tap equalization per outer sub-channel.

To proceed, we assume the media to be time-invariant over the duration of the prototype pulse $g(t)$. Then, we can run filtering with pulses that are matched to the sub-channel transmit filters. Assuming knowledge of the time and frequency offsets (that have in practice to be estimated), the sequence of samples at the matched filter output of inner sub-channel $\tilde{k} = 0, \dots, M-1$, of user $\tilde{u} = 1, \dots, N_U$, and receive antenna $r = 0, \dots, N_R - 1$, can be written as

$$z_{inner}^{\tilde{u}, \tilde{k}, r}(mT_0) = \sum_{i \in \mathbb{Z}} y(iT + \Delta t_{\tilde{u}, \tilde{k}}) g^*(iT - mT_0) e^{-j[\frac{2\pi}{M} i\tilde{k} + 2\pi \Delta f_{\tilde{u}, \tilde{k}} iT]} \quad (7)$$

$$= \sum_{u=1}^{N_U} \sum_{t=0}^{N_T-1} \sum_{k=0}^{M-1} \sum_{l \in \mathbb{Z}} b^{u,k,t}(lT_0) g_{EQ}^{u,k,t,r}(mT_0 - lT_0; mT_0) + \eta^{\tilde{u}, \tilde{k}, r}(mT_0)$$

$$g_{EQ}^{u,k,t,r}(lT_0; mT_0) = \sum_{n \in \mathbb{Z}} \sum_{i \in \mathbb{Z}} g(nT + lT_0 - mT_0) g^*(iT - mT_0)$$

$$\times g_{ch}^{u,t,r}(iT - nT - \Delta t_{u,k} + \Delta t_{\tilde{u}, \tilde{k}}; mT_0 + \Delta t_{\tilde{u}, \tilde{k}}) e^{j[2\pi(\frac{nk - i\tilde{k}}{M} + (\Delta f_{u,k} - \Delta f_{\tilde{u}, \tilde{k}})iT) + \phi_{u,k}]} \quad (8)$$

with $\hat{\phi}_{u,k}$ being an appropriate phase offset. Assuming a tapped delay line channel, its impulse response can be written as

$$g_{ch}^{u,t,r}(iT - \Delta t_{u,k} + \Delta t_{\tilde{u}, \tilde{k}}; mT_0 + \Delta t_{\tilde{u}, \tilde{k}}) = \sum_{p \in P} \alpha_p^{u,t,r}(mT_0) \delta(iT - pT - p_{u,k}T + p_{\tilde{u}, \tilde{k}}T) \quad (8)$$

where $p_{u,k} = \lfloor \Delta t_{u,k} \rfloor$, $\alpha_p^{u,t,r}(mT_0)$ are the tap amplitudes, and P is the set of tap delays. Thus, the equivalent impulse response becomes

$$g_{EQ}^{u,k,t,r}(lT_0; mT_0) = \sum_{p \in P} \alpha_p^{u,t,r}(mT_0) \sum_{i \in \mathbb{Z}} g(iT - pT - p_{u,k}T + p_{\tilde{u}, \tilde{k}}T + lT_0 - mT_0) g^*(iT - mT_0) e^{j[\frac{2\pi}{M}(ik - pk - i\tilde{k}) + 2\pi(\Delta f_{u,k} - \Delta f_{\tilde{u}, \tilde{k}})iT + \phi_{u,k}]} \quad (9)$$

Using Parseval theorem it can be shown that with the conditions

$$\mathbf{a.} \quad |G(f)| = 0 \quad \text{for} \quad |f| > (1 + \alpha_1)/2T_0, \quad \mathbf{b.} \quad |\Delta f_{u,k}| \leq \alpha_2/2T_0,$$

relation (9) differs from zero only for $k = \tilde{k}$. In other words the inner sub-channels have zero cross-correlation, and they do not overlap, i.e., there is no inter-channel interference (ICI). In such conditions that can be met with the appropriate system design (see Section IV), we obtain

$$z_{inner}^{\tilde{u}, \tilde{k}, r}(mT_0) = \sum_{u=1}^{N_U} \sum_{t=0}^{N_T-1} \sum_{k=0}^{M-1} b^{u,k,t}(lT_0) g_{EQ}^{u,k,t,r}(mT_0 - lT_0; mT_0) + \eta^{\tilde{u}, \tilde{k}, r}(mT_0). \quad (10)$$

Thus, the matched filter output sample experiences multiple access interference (MAI) only if the same sub-channel is assigned to more than one user. However, ISI is in general present, and the N_T spatial channels overlap due to simultaneous transmission of signals by multiple antennas. Therefore, if we assume to assign distinct tones to distinct users which can be done in a given cell (sector), (10) becomes

$$z_{inner}^{\tilde{u}, \tilde{k}, r}(mT_0) = \sum_{t=0}^{N_T-1} \sum_{p=0}^{N_p} \beta_p^{\tilde{u}, \tilde{k}, t, r}(mT_0) b^{\tilde{u}, \tilde{k}, t}(mT_0 - pT_0) + \eta^{\tilde{u}, \tilde{k}, r}(mT_0) \quad (11)$$

$$\beta_l^{\tilde{u}, \tilde{k}, t, r}(mT_0) = \sum_{p \in P} \alpha_p^{\tilde{u}, t, r}(mT_0) \kappa_g(lT_0 - pT) e^{-j\frac{2\pi}{M} p\tilde{k}} e^{j\hat{\phi}_{\tilde{u}, \tilde{k}}} \quad (11)$$

where $\kappa_g(mT) = \sum_i g(iT) g^*(iT - mT)$ is the prototype pulse autocorrelation, and N_p is the number of T_0 spaced inner channel taps $\beta_l^{\tilde{u}, \tilde{k}, t, r}(mT_0)$. Thus, the inner sub-channel \tilde{k} of user \tilde{u} exhibits ISI but sees only the superposition of the signals that are transmitted by its N_T antennas. If we do not use the

outer modulator we need to accomplish data detection at this stage. Since there is ISI, sub-channel space-time equalization is required [8]. However, depending upon the sub-channel bandwidth, the number of taps N_p is small. Optimal and simplified equalization schemes are described in [10], [11], [12].

C. Outer ST-O-DMT Demodulation

In order to completely remove the inner sub-channel ISI, and to orthogonalize the spatial channels we use the outer ST-OC-DMT modulator. In what follows we describe the demodulation process that takes place for each inner-sub-channel at the output of the FMT front-end.

Let us start from (11), and let us collect the received signal samples at the FMT front-end output of receive antenna r and inner sub-channel \tilde{k} , into blocks of N samples that we denote as

$$z_{inner}^{\tilde{u},\tilde{k},r}(nT_0 + lNT_0) \quad \text{for } l = -\infty, \dots, \infty, \quad n = 0, \dots, N-1. \quad (12)$$

If we combine (11)-(12) with (4), under the conditions

- c. μT_0 larger than the inner sub-channel time dispersion $N_p T_0$,
- d. time-invariant channel over a window of length NT_0 ,

for the samples of index $n = \mu, \dots, N-1$ the following relation holds true

$$z_{inner}^{\tilde{u},\tilde{k},r}(nT_0 + lNT_0) = \sum_{t=0}^{N_T-1} \sum_{p=0}^{N_p} \beta_p^{\tilde{u},\tilde{k},t,r}(lNT_0) b^{\tilde{u},\tilde{k},t,n-p}(lNT_0) + \eta^{\tilde{u},\tilde{k},r}(nT_0 + lNT_0). \quad (13)$$

Now, for each receive antenna, and inner sub-channel, ST-OC-DMT demodulation is accomplished by dropping the cyclic prefix (the samples of the l -th block corresponding to index $n = 0, \dots, \mu-1$), and applying an M_2 -point FFT to obtain

$$z_{outer}^{\tilde{u},\tilde{k},k',r}(lNT_0) = H^{\tilde{u},\tilde{k},k',r}(lNT_0) a^{\tilde{u},\tilde{k},k'}(lNT_0) + n^{\tilde{u},\tilde{k},k',r}(lNT_0) \quad (14)$$

$$H^{\tilde{u},\tilde{k},k',r}(lNT_0) = \sum_{t=0}^{N_T-1} \sum_{p=0}^{N_p} \beta_p^{\tilde{u},\tilde{k},t,r}(lNT_0) e^{-j\frac{2\pi}{M_2}(p+t\delta)k'} \quad (15)$$

for $k' = 0, \dots, M_2-1$. That is, the FFT output of index k' ,

$z_{outer}^{\tilde{u},\tilde{k},k',r}(lNT_0)$, is given by the superposition of noise with the data symbol transmitted on the same outer sub-channel. The data symbol is weighted by an equivalent channel transfer function $H^{\tilde{u},\tilde{k},k',r}(lNT_0)$. Therefore, each FFT output sees a single-input single-output flat faded channel, and the multiple transmit antenna system is transformed into a single transmit antenna system that is characterized by the transfer function (15).

If the symbols $a^{\tilde{u},\tilde{k},k'}(lNT_0)$ belong to the PSK/QAM constellation, data decisions are made after maximal ratio combining (MRC) of the N_R received signals (14). However, if data spreading is used we still need to go through another stage before making data decisions. This is illustrated in the next sub-section.

It should be noted that without channel coding or DS data spreading no diversity exploitation is possible, since the con-

catenation of the outer, and inner modulators generates for user u , $L = M_2 M_u$ non-overlapping flat faded channels. It can be proved that if the $N_T N_p$ channel taps $\beta_p^{\tilde{u},\tilde{k},t,r}$ (for $p = 0, \dots, N_p-1$, and $t = 0, \dots, N_T-1$) are independent, then the rank of the $M_2 \times M_2$ correlation matrix whose entries are $R^{k',k''} = E[H^{\tilde{u},\tilde{k},k',r}(lNT_0) H^{\tilde{u},\tilde{k},k'',r*}(lNT_0)]$ is $N_T N_p$. Thus, the rank of the space-time inner sub-channel remains unchanged. In Section V we report numerical results to show the performance improvement that is achievable with outer data spreading.

D. Data Despreading

When DS data spreading is used, if we substitute (5) in (15), the output of the outer O-ST-CP-DMT demodulator reads

$$z_{outer}^{\tilde{u},\tilde{k},k',r}(lNT_0) = H^{\tilde{u},\tilde{k},k',r}(lNT_0) \sum_{i=0}^{L-1} \tilde{a}^{u,i}(lNT_0) c(i, \tilde{k}M_2 + k') + n^{\tilde{u},\tilde{k},k',r}(lNT_0). \quad (16)$$

To accomplish data despreading we can pursue either a zero forcing (ZF), or a minimum mean square error (MMSE) approach [3]. Herein, we consider the former scheme for its simplicity, although the latter scheme yields better performance. Assuming the deployment of N_R receive antennas, with ZF detection and antenna combining, we obtain the following output signal (under conditions c. and d. above)

$$z_{despr}^{\tilde{u},i}(l) = \sum_{\tilde{k}=0}^{M_u-1} \sum_{k'=0}^{M_2-1} \frac{z_{outer}^{\tilde{u},\tilde{k},k',r}(lNT_0) H^{\tilde{u},\tilde{k},k',r}(lNT_0)^*}{\sum_{r=0}^{N_R-1} |H^{\tilde{u},\tilde{k},k',r}(lNT_0)|^2} c^*(i, \tilde{k}M_2 + k') \quad (17) = \tilde{a}^{\tilde{u},i}(lNT_0) + w^{\tilde{u},i}(lNT_0).$$

Thus, we perfectly equalize the channel, i.e., we get the transmitted PSK/QAM data symbols $\tilde{a}^{\tilde{u},i}(lNT_0)$, $i=0, \dots, L-1$, plus an additive Gaussian noise term that has zero mean, and variance

$$\sigma_w^2 = E[|w^{\tilde{u},i}(lNT_0)|^2] = \sigma_n^2 \sum_{\tilde{k}=0}^{M_u-1} \sum_{k'=0}^{M_2-1} \left(\sum_{r=0}^{N_R-1} |H^{\tilde{u},\tilde{k},k',r}(lNT_0)|^2 \right)^{-1} \quad (18)$$

assuming $n^{\tilde{u},\tilde{k},k',r}(lNT_0)$ to be independent zero mean Gaussian with variance σ_n^2 . It is known that ZF detection is characterized by noise enhancements. However, we have found that such an effect is smoothed with receive antenna diversity, and the performance improvement that is achievable with frequency and transmit diversity exploitation is sensible (Section V). Clearly, if the conditions s. and d. of Section III.C are not perfectly fulfilled, the output of the ZF detector exhibits some extra interference contribution.

IV. SYSTEM DESIGN AND PARAMETER CHOICE

As we said above, the system design pursues the goal of orthogonalizing asynchronous uplink users. We do not force the users to adjust their timing, and carrier frequency such that they appear the same at the base station. We assume a much softer synchronization approach that is based on simply mak-

ing the users adjusting their timing based on the downlink frame. In such a case, at the base station distinct users signals still experience time offsets and carrier frequency offsets relatively to the base station reference signal. The time offsets are equal to the two-way propagation delay, i.e., $\Delta t(r) = 2r/c = 6.67 \mu\text{s}/\text{km}$, while the frequency offsets are equal to the frequency Doppler shift due to the mobiles movements, i.e., $\Delta f(v) = v f_c / c = 0.93 \text{ Hz}/\text{GHz}/\text{km}/\text{h}$. For instance with up to 5 km cell radius $\Delta t \leq 33.3 \mu\text{s}$, while with $f_c = 2.5 \text{ GHz}$, and $v \leq 200 \text{ km}/\text{h}$ we have $\Delta f \leq 463 \text{ Hz}$. Indeed we could also deploy transmit carrier frequency adjustment, i.e., compensation of the frequency offset at the transmitter at the expense of increased complexity [16].

Now if we turn our attention to the propagation media, the coherence bandwidth, and the coherence time are related to the rms delay spread σ_τ , and the maximum Doppler spread f_D , through the following relations [7] $B_{ch} = 1/(2\pi\sigma_\tau)$, and $T_{ch} = 9/(16\pi f_D)$. With $\sigma_\tau \leq 10 \mu\text{s}$, and $f_D \leq 465 \text{ Hz}$, we obtain that $B_{ch} \geq 15.9 \text{ kHz}$, and $T_{ch} \geq 0.38 \text{ ms}$. Keeping this in mind, we choose a number of inner sub-carriers such that a tradeoff in terms of large coherence bandwidth and coherence time with respect to the transmission parameters is safely fulfilled. We also have to emphasize that since the users are frequency multiplexed, a sufficient number of tones have to be chosen to grant an appropriate level of granularity in terms of simultaneously active users and transmission rate per user.

A. System Example with $W=3.84 \text{ MHz}$ Bandwidth

As an example, we report system parameters in Table II assuming transmission at 3.84 MHz (as in UMTS). To allow system flexibility we can support both frequency and time multiplexing in a dynamic fashion which is handled by the MAC layer. That is, simultaneous transmission is performed across distinct tones, thus supporting up to 64 users. The minimum burst duration is 0.3817 ms. Further, each tone can be shared in a time division mode every MAC frame that comprises a certain number of bursts.

The air-interface can be parameterized to work with wider bandwidths.

B. Avoiding the Outer Modulator in High Doppler Scenarios

The deployment of the O-ST-CP-DMT modulators allows for simple one-tap equalization in certain mobility conditions. For high mobility users, condition *d.* above might not be fulfilled. For such users we can avoid using the outer modulator. Instead, we perform adaptive sub-channel equalization directly at the output of the FMT front-end. Such an equalizer can have reasonably low complexity since the number of inner channel taps is definitely small. In the rare event that perfect users orthogonalization is not possible, some ISI, ICI, and MAI can be present, e.g., when the frequency offsets exceed the chosen frequency guard, the delay spread exceeds the one used for the system design, the Doppler spread is high. To optimize performance multicarrier multiuser detection can be used. Details can be found in [10], [12].

$M = 64$	Number of tones of inner modulator
$1/MT = W/M = 60 \text{ kHz}$	Inner Sub-channel bandwidth
$\alpha = \alpha_1 + \alpha_2 = 0.125 + 0.02 = 0.145$	Roll-off + Guard factor inner modulator
$1/T_0 = 1/MT/(1+\alpha) = 52.4017 \text{ kHz}$	Inner Sub-channel transmission rate
$T_0 = 19.083 \mu\text{s}$	Inner Sub-channel symbol period
$N_{LS} = 20$	Minimum number of symbols per burst
$T_B = 20T_0 = 0.3817 \text{ ms}$	Minimum burst duration
$N_U = 64$	Maximum number of users per frame
$R_{TOT} = 6.707 \text{ Mb/s}$ 4-PSK	Aggregate max transmission rate per sector with inner modulator only
$R_{TOT} = 13.415 \text{ Mb/s}$ 16-QAM	
$M_2 = 16$	Number of tones outer modulator
$\mu = 4$	Cyclic prefix length
$1/(M_2 + \mu)T_0 = 2.62 \text{ kHz}$	Outer sub-channel transmission rate
$R_{TOT} = 5.366 \text{ Mb/s}$ 4-PSK	Aggregate max transmission rate per sector with outer modulator
$R_{TOT} = 10.731 \text{ Mb/s}$ 16-QAM	

C. Increasing Performance with Frequency Hopping

To obtain further diversity, and interference averaging benefits it is possible to use also frequency hopping. It has to be emphasized that frequency hopping requires hopping and frame synchronization across users in order to preserve orthogonality. However, frame synchronization is not required if the number of frequency bins (inner sub-channels) M is at least equal to $2N_U$, so that users can hop to free bins. Details on frequency hopping can be found in [9].

D. Channel Coding

For space limitations, we do not discuss channel coding. A reasonable and popular choice is to use bit-interleaved codes [3], [2].

V. SYSTEM PERFORMANCE

We report in Fig. 3, and Fig. 4 the average BER performance for the system whose parameters are given in Table II. We assume 4-PSK modulation, s.r.r.c sub-channel pulses for the FMT inner modulator with roll off $\alpha_1=0.125$. The O-ST-CP-DMT outer modulator is combined with Walsh-Hadamard DS spreading. $N_U=64$ users deploy a single and distinct inner sub-channel. They are time asynchronous, and have $\Delta f \leq 463 \text{ Hz}$. Both flat and frequency selective Rayleigh fading are considered. In the latter case, the fading is slow (static over the duration T_B of a burst), the channel taps $\alpha_p^{i,t,r}(mT_B)$ are assumed to be independent, and to have an exponential power delay profile with rms delay spread $\sigma_\tau=2 \mu\text{s}$. The resulting channel has duration $39T$. Further, we assume double receive diversity with ZF detection, and ideal knowledge of the channel, and time/frequency offset.

The curves show the diversity effect as a function of the number of transmit antennas, and the length of the spreading code. The E_b/N_0 has been normalized by the number of transmit antennas, and includes the penalty due to the cyclic prefix used in the outer O-ST-CP-DMT modulator. Curves labelled with *outer unspread* report BER computed at output of the outer demodulator without DS spreading. Curves labelled with *outer+spread single* report the BER at the output of the outer demodulator with DS spreading over $M_2=16$ outer channels (i.e., over the spectrum occupied by a single inner sub-channel that is assigned to a single user). In both cases the BER is averaged over all users, and equals the BER that would be

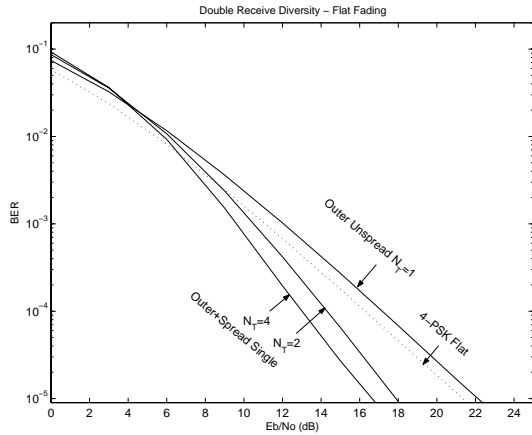


Fig. 3. Average BER performance in flat Rayleigh fading with double receive diversity, and with $N_T = 1, 2, 4$ transmit antennas.

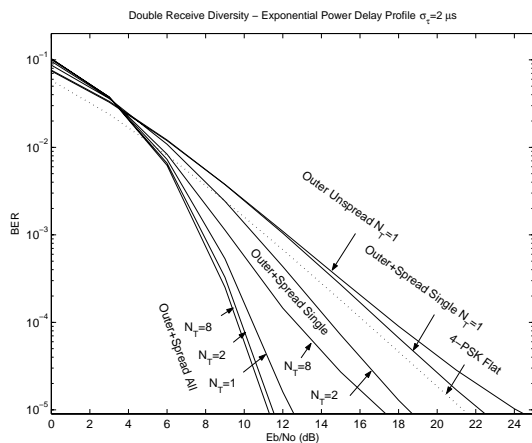


Fig. 4. Average BER performance in frequency selective Rayleigh fading with double receive diversity, and with $N_T = 1, 2, 8$ transmit antennas.

achieved with frequency hopping across the sub-channels [9]. Curves labelled with *outer+spread all* show the BER at the output of the outer demodulator with DS spreading over all $M_2M=1024$ outer channels. In this case a single user is present, and is assigned with all inner channels in the system. As a reference, we plot also the BER of 4-PSK in flat fading with double receive diversity.

In Fig. 3 we consider a flat fading channel. As the figure shows, the performance improvement as the number of transmit antennas increases, is sensible.

In Fig. 4 we consider frequency selective fading. The performance improvement as N_T increases is significant for the *outer+spread single* case, while is lower when spreading takes place over all sub-channels because the frequency diversity offered by the overall system bandwidth is already high. The error floors at high SNR are mainly due to the uncompensated ISI that exceeds the outer modulator cyclic prefix of duration $4T_0$. In general, the frequency diversity gain is a function of the number of inner sub-channels that are assigned to a given user. Thus, the use of multiple transmit antennas with DS spreading yields higher incremental gains for users that are allocated to a small number of inner sub-channels. In this case frequency hopping is also beneficial [9]. Further improvements are possible

with other detection approaches, e.g., MMSE detection.

VI. CONCLUSIONS

We have presented an air-interface approach for uplink wireless communications. It is based on concatenated FMT modulation, and O-ST-CP-DMT modulation with multiple transmit antennas and direct sequence data spreading. It can also include frequency hopping to achieve diversity and interference averaging benefits [9]. We have reported an analysis to determine the conditions under which the multiuser multiple antenna system can be orthogonalized such that neither MAI nor ICI and ISI arise at the receiver side. Guidelines, for system design have been described. Finally, numerical results have been shown to highlight the performance gains that can be obtained as a function of the number of transmit antennas.

VII. REFERENCES

- [1] G. Cherubini, E. Eleftheriou, S. Ölçer, J. Cioffi, "Filter bank modulation techniques for very high-speed digital subscriber lines", *IEEE Commun. Magazine*, pp. 98-104, May 2000.
- [2] A. Dammann, R. Raulefs, G. Auer, G. Bauch, "Comparison of space-time block coding and cyclic delay diversity for broadband mobile radio air interface", Proc. of WPMC 2003, vol. 2, pp. 411-415, October 2003.
- [3] S. Kaiser, "OFDM code division multiplexing in fading channels", *IEEE Trans. Comm.*, pp. 1266-1273, August 2002.
- [4] S. Kaiser, W. Krzymien, "Performance effects of the uplink asynchronism is a spread spectrum multi-carrier multiple access system", *European Trans. on Telec.*, pp. 399-406, July-August 1999.
- [5] I. Lee, A. Chan, W. Sundberg, "Space-time bit-interleaved coded modulation for OFDM systems in wireless LAN applications", *IEEE Proc. ICC '03*, pp. 3413-3417, May 2003.
- [6] Z. Liu, Y. Xin, G. Giannakis, "Space-time frequency coded OFDM over frequency selective fading channels", *IEEE Trans. Signal Proc.*, pp. 2465-2475, October 2002.
- [7] R. Steele, "Mobile Communications", Pentech Press Ltd, 1992.
- [8] A. Tonello, "Orthogonal space-time discrete multitone and space-time filtered multitone coded architectures", Proc. of IEEE VTC 2004 Spring, Milan, Italy, May 2004.
- [9] A. Tonello, A. Assalini, "An asynchronous multitone multiuser air interface for high-speed uplink communications", Proc. of IEEE VTC 2003 Fall, Orlando, USA, September 2003.
- [10] A. Tonello, "Asynchronous multicarrier multiple access: optimal and sub-optimal detection and decoding", *Bell Labs Technical Journal* vol. 7 n. 3, pp. 191-217, February 2003.
- [11] A. Tonello, "MIMO MAP equalization and turbo decoding in interleaved space-time coded systems", *IEEE Trans. on Comm.*, pp.155-160, February 2003.
- [12] A. Tonello, "Multiuser detection/decoding in asynchronous multitone multiple access systems", *Proc. of IEEE WPMC 02*, Honolulu, pp. 1242-1246, October 2002.
- [13] A. Tonello, S. Pupolin, "Performance of single user detectors in multitone multiple access asynchronous communications", *Proc. of IEEE VTC 02-Spring*, pp. 199-203, May 2002.
- [14] A. Tonello, S. Pupolin, "Discrete multi-tone and filtered multi-tone architectures for broadband asynchronous multi-user communications", *Proc. of WPMC 01*, Aalborg, pp. 461-466, September 2001.
- [15] A. Tonello, N. Laurenti, and S. Pupolin, "Analysis of the uplink of an asynchronous DMT OFDMA system impaired by time offsets, frequency offsets, and multi-path fading", *Proc. of IEEE VTC 00-Fall*, Boston, pp.1094-1099, September 2000.
- [16] J. van de Beek, P.O. Borjesson, et al. "A time and frequency synchronization scheme for multiuser OFDM", *IEEE JSAC*, pp. 1900-1914, Nov. 1999.
- [17] C. Yui, R. Cheng, K. Ben Letaief, R. Murch, "Multiuser OFDM with adaptive subcarrier, bit, and power allocation", *IEEE JSAC*, pp. 1747-1758, October 1999.